Delaunay Lofts: A Biologically Inspired Approach for Modeling Space Filling Modular Structures

Sai Ganesh Subramanian[a], Mathew Eng[b], Vinayak R. Krishnamurthy[a,*], Ergun Akleman[b]

[a] *J. Mike Walker '66 Department of Mechanical Engineering*
Texas A& M University, College Station, Texas, 77843
[b] *Department of Visualization & Computer Science and Engineering*
Texas A& M University, College Station, Texas, 77843

Abstract

In this paper, we present a simple and intuitive approach for designing space filling tiles in 3D space. Our approach is inspired by "scutoids" — shapes that were recently reported to occur in epithelial cells due to topological changes between the extremal (apical and basal) surfaces of epithelia. Drawing from this discovery, we develop the theoretical and computational foundations leading to a generalized procedure for generating *Delaunay Lofts* — a new class of scutoid-like shapes. Given two extremal surfaces, both with Delaunay diagrams, Delaunay Lofts are shapes that result from Voronoi tessellation of all intermediate surfaces along the curves joining the vertices of Delaunay diagrams that defines the extremal tessellations. This, combined with the use of wallpaper symmetries allows for intuitive design of complex space filling regular and semi-regular tilings in 3D space.

Keywords: Tessellation of Space, Space Filling Structures, 3D Tile Design

1. Introduction

1.1. Problem & Context

Shell and volume structures are usually composed of regular prisms (such as rectangular blocks) since they are relatively easy to manufacture and are widely available. Unfortunately, reliance on regular prisms inherently constrains our design space for obtaining reliable and robust structures (1; 2; 3; 4; 5). Architects currently investigate many other types of space filling modules, but their investigations are not usually systematic and focus on only a small number of known building blocks (6). There is a need for formal approaches that enable the design and intuitively *control* of a wide variety of modular and tile-able building blocks.

In this paper, we introduce such a conceptually simple and formal approach to design *unconventional* building blocks that *can be mass-produced and result in a space filling packing*. Our approach is based on a layer-by-layer interpolation of 2D tiles using Voronoi decomposition along the third dimension in a given 3D domain. We call these building blocks *Delaunay Lofts*, since interpolation process is similar to Lofting but is based on Voronoi partitioning of each 2D interpolated domain. Such a partitioning allows for changing the topology of the shape unlike extrude or sweep operations.

1.2. Inspiration & Approach

Until recently, the biological community assumed that cells that packed together to form thin structures (such as organ skin) were primarily prism-like shapes. This view was recently updated through the discovery of "scutoids" — shapes that frequently occur in animal skin-cells (7). The formation of these thin (2.5D) structures can be viewed as a topology changing interpolation through edge-collapse or vertex-split operations between quadrilaterals, pentagons and hexagonal faces of any given tessellation.

Inspired by this new discovery, we first offer a view that provides a *dual* version of this explanation. We observe that scutoids could be formed by a Voronoi partitioning of a shell into regions based on distance to a set curves along the thickness of the shell. This dual explanation is theoretically useful since (1) it provides a well-defined process to compute the boundaries of resulting structures; and (2) it is able to naturally create curved boundaries that is expected for resulting structures.

*Corresponding author: Email: vinayak@tamu.edu

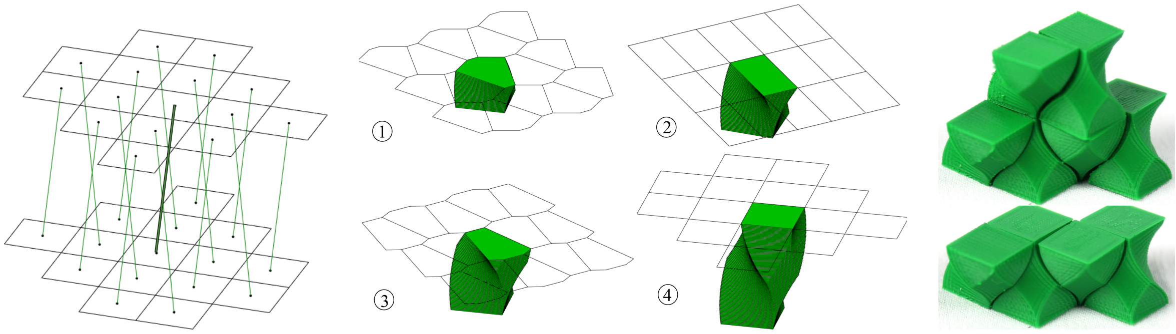

(a) The control lines that interpolates top and bottom Voronoi sites. *(b) Construction process of Delaunay Lofts demonstrating tilings in four different layers.* *(c) 3D-Printed space filling Delaunay Lofts.*

Figure 1: The process of construction of Delaunay Lofts. We first creates a set of control curves as shown in (a). Control curves that interpolates Voronoi sites are shown in green. Voronoi sites are black dots. We, then, compute Voronoi decomposition in set of layers as shown in (b). We construct Delaunay Lofts by interpolating the Voronoi polygons. The resulting Delaunay Lofts in this case are shown in (c).

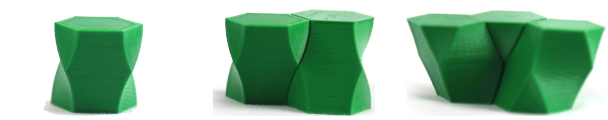

(a) A Delaunay Loft. *(b) Two tiles.* *(c) Three tiles.*

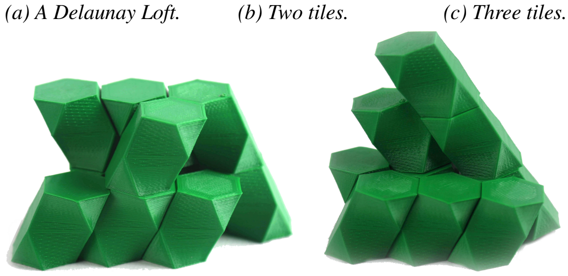

(d) Ten tiles. *(e) Ten tiles.*

Figure 2: An example of single Delaunay Loft tile that can fill both 2.5D and 3D space. This tile is created as an interpolation of three layers of tilings, namely (1) a regular hexagonal; (2) a square and; (3) another regular hexagonal tilings, which is translation of the first hexagonal tiling. The interpolating control lines are straight lines and we do not really interpolate regular rectangular tiles. They are automatically produced.

From the shape modeling point of view, this dual explanation provides a simple yet powerful conceptual framework that can be used to model and design a wide variety of modular shell structures. Users can simply provide *a set of control curves as Voronoi sites to obtain a decomposition of a thin plate*. Even straight lines can result in interesting structures with curved boundaries. Based on this explanation, we have developed a set of simple and intuitive procedures to design a wide variety of unconventional — and also non-intuitive — building blocks.

Figures 1 and 2 show examples of such non-intuitive space filling tiles that are designed using our procedure. In Figure 1, one way to reason regarding the extremal tilings is to view the bottom layer as a translated version of regular square grid in the top layer. Sweeping of a square profile through translation is normally expected to result in a prism with planar parallelogram faces. However, tilings are not standard single objects. We can obtain a rigid body transformation of a tiling in more than one way. Figure 1(b) shows how the tiling is interpolated in this particular case. As it can be seen in Figure 1(b), the motion of Voronoi sites produces hexagonal grids, which causes a change of 1D topology from quadrilateral to hexagon and back to quadrilateral. This topological change is clearly visible in the 2.5D tilings shown in Figure 1 by triangles resulting from edge collapse — a change that is also noted by the researches on biological cell packing (7). Further, note that these triangles are not planar since they are naturally created as a by-product of Voronoi decomposition. Since the top and bottom tilings are rigid transformation of each other, these are 3D space filling shapes as shown in Figures 1 and 2.

1.3. Contributions

We make three main contributions in this work. First, we develop a generalized approach for constructing space-filling tilings in 3D space. This approach is based on two key principles, the first being the use of higher-dimensional sites (lines instead of points) for Voronoi decomposition of 3D space and the second being the use of wallpaper symmetries to obtain repeatable tilings. Our second contribution is a method for direct control of the topological change in Delaunay Lofts. Lastly, our contribution is the algorithm to practically construct Delaunay Lofts in real-time at arbitrary resolutions without resorting to the voxelization of a domain in 3D space. This is based on distance functions induced by lines on a layer-by-layer basis.

The examples in Figures 1 and 2 demonstrate the power of our approach for designing unusual space filling structures with a simple input — a set of lines constructed based on known symmetries. Despite the apparent complexity of the shapes themselves, the procedure to generate a complete class of such shapes is rather simple. In the rest of the paper, we first provide the biological inspiration and theoretical foundations of this approach in sections 2 and 3. Section 4 introduces our methodology to construct these shapes. We then demonstrate the results obtained by our approach in a systematic manner in section 5. Finally, we discuss the implications of this approach and potential extensions in sections 6 and 7.

2. Related Work

A space filling shape is a cellular structure whose replicas together can fill all of space watertight, i.e. without having any voids between them (8). Equivalently, a space filling shape is a cellular structure that can be used to generate a tessellation of space (9). While 2D tessellations and space filling shapes are relatively well-understood (subsection 3.4), problems related to 3D tessellations and space filling shapes are interesting and have applications in a wide range of areas from chemistry and biology to engineering and architecture (8).

A well-known anecdote to demonstrate the difficulty of 3D tessellations is that Aristotle claimed that the tetrahedron can fill space. Several efforts were made to prove his claim (10) only to find that cube is the only space filling Platonic solid (11). Goldberg exhaustively catalogued many of known space-filling polyhedra with a series of papers from 1972 to 1982 such as (12; 13; 14). There are only eight space-filling convex polyhedra and only five of them have regular faces, namely the triangular prism, hexagonal prism, cube, truncated octahedron (15; 16), and Johnson solid gyrobifastigium (17; 18). It is also interesting that five of these eight space filling shapes are "primary" parallelohedra (19), namely cube, hexagonal prism, rhombic dodecahedron, elongated dodecahedron, and truncated octahedron.

There have been many works in interpolations of tilings in 2D space(20; 21; 22; 23). Recently, there has been interest in the mechanical characterization of 3D printed 2D tilings in the context of "sheet materials" as well (24). In this case, the sheet material is only a thin extrusion of a two-dimensional tiling. Two interesting cases of 2D tilings relevant to our approach are those presented by Kaplan (25) showing a wide variety of artistic patterns using specific Voronoi site configurations and Rao (26) that show a systematic construction of 2D pentagonal tilings. In fact our work, in a sense, expands on these two works to move beyond tilings in 2D space to a rich design space of tilings in 3D space.

In this paper, we have developed an approach to construct non-polyhedral space filling shapes. Our approach, which can be considered as a generalization of parallelohedra, is inspired by a recent discovery by Gómez-Gálvez et al.(7) who observed that a simple polyhedral form, which they call *"scutoids"*, commonly exists in epithelia cells in the formation of skin cells. They demonstrated that having this polyhedral form in addition to prisms provides a natural solution to three-dimensional packing of epithelial cells. In skin cells, the top (apical) and bottom (basal) surfaces of the cellular structure are Voronoi patterns (as these occur frequently due to physical constraints) (27). Gómez-Gálvez et al. observed that the fundamental problem of packing occurs when the polygonal shapes at apical and basal surfaces do not match (e.g. pentagonal top and hexagonal bottom) leading to topological shift and resulting in scutoids.

The literature on this discovery shows the occurrence of scutoids and provides some statistical information of when and how they form (7; 28; 29; 30) (Figure 3). The reason why these shapes occur in nature is that they are the sole enablers for a space filling packing on the skin cells. These shapes, as discussed earlier, are based on a special type of (topological) interpolation between 2D tiling patterns. These 2D tiling patterns typically contain simple polygonal shapes such as hexagons and pentagons that appear on many natural structures.

The Figure 3(a) demonstrates a usual depiction of the originally discovered scutoid structures obtained by edge-collapse or vertex-split operations between quadrilaterals, pentagons and hexagonal faces. This view results in non-planar pentagons or hexagons with straight boundaries as shown in the Figure 3(a), but it does not provide any well-defined process to fill inside of these non-planar faces. Our approach is to produce space filling tiles using Delaunay diagrams with wallpaper symmetries. For instance, by choosing a stack of regular or semi-regular tilings as Delaunay triangulations for the interpolation of vertices, we obtain a set of control curves that produces space filling tiles. If the top and bottom tilings are rigid transformations of each other, this process can also produce 3D space filling shapes.

Delaunay Lofts generalize scutoid-producing biological process and can create a set of shapes that contains the aforementioned scutoids and many other shapes that can pack together in a space filling manner with each other, which we call Delaunay Lofts (Figure 3(b) and (c)). By simply assembling several of these new space filling Delaunay Lofts, several types of shapes can be computationally designed and physically manufactured for mechanical (structures), architectural (tilings), and educational (puzzles) purposes.

Our approach to obtain space filling structures, in general, can be considered 3D Voronoi decomposition of a set of curves that is closed under symmetry operations. The resulted Voronoi shapes in this case are guaranteed to be space filling. We note that our approach is also in sync with Delaunay's original intention for the use of Delaunay diagrams. He was the first to use symmetry operations on points and Voronoi diagrams to produce space filling polyhedra, which he called Stereohedra (31; 32). Our approach can be viewed as an idea that stems from his general conceptual framework. We, therefore, called our approach Delaunay Lofts.

When using points, construction of 3D Voronoi decomposition is relatively simple since distances to points guarantee to produce planar faces. On the other hand, when we use curves or even straight lines Voronoi decomposition can produce curved faces which, in fact, makes our method interesting. However, having curved faces significantly complicates the algorithms to construct 3D Voronoi decomposition in high resolution. We, therefore, choose to deal with a subset of this general problem by: (1) decomposing the 3D domain into thin rectangular structures that consist of a discrete set of z-constant planar layers and (2) using only 2D symmetry operations based on wallpaper patterns. The next section provides theoretical foundations to develop such practical methods to construct Delaunay Lofts.

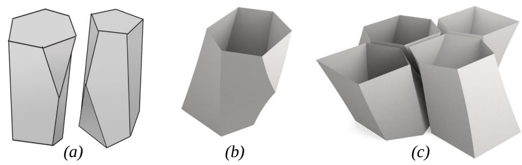

Figure 3: A comparison of the original scutoid discovered by Gomel-Gomez et al. (7) (a) with the one generated by our method (b) shows the difference between the interfacing boundaries between two different blocks. Note that not more than 4 of these shapes can be fit together which means these structures are not repeatable and cannot fill the space (c).

3. Theoretical Foundations

In this section, we provide the basic foundations for our approach. All the information in this section is well-known. We only provide it to establish a context for our approach. This background will also provide a foundation for the development of algorithms to construct space-filling tiles in 3D space.

3.1. Fundamental Domain

In this paper, we present our approach as the decomposition of a 3-torus that is given as a repeated cubical domain, $[0, 1]^3$ (33) as its fundamental domain. In other words, $x \equiv x - \lfloor x \rfloor$, $y \equiv y - \lfloor y \rfloor$, and $z \equiv z - \lfloor z \rfloor$ where the floor operator ($\lfloor a \rfloor$) gives the greater integer less than or equal to a. This gives us a regular tessellation of 3D space. We usually assume that z does not repeat and $0 \leq z \leq 1$ represents a shell, i.e. a 2.5D structure. We further assume that curved shapes are obtained by a deformation of this domain such as a tensor product free-form volume that is defined on this cubical domain (34; 35). Such deformations are, of course, not straightforward, but we purposely provide our presentation using this simple domain to simplify our explanation without loss of generality.

3.1.1. Domain Decomposition using Control Curves

Given the fundamental domain, our approach is simply to compute a Voronoi decomposition of this cubical domain into the regions based on distance to a set of curves given in the form of $(x_i = f_{i,x}(z), y_i = f_{i,y}(z))$, where $i = 0, 1 \ldots$, n. Since these curves intersect any given $z = c$ constant plane only once, with a well-defined distance function, the decomposition of the 3D domain can be simplified as a sequence of 2D Voronoi decomposition at each planar layer, $z = c$, based on the distance to a set of points $(x_i = f_{i,x}(c), y_i = f_{i,y}(c))$ (See subsection 3.2).

3.1.2. Interpolation Curves

We further assume that each of these control curves are interpolations of a set of control points given $z = c_j$ as $(x_{i,j}, y_{i,j}, c_j)$. We simply choose these points to obtain any desired Voronoi decomposition in any given planar layer. Using these points as control points of the curves we can obtain any desired Voronoi decomposition. For interpolation, there is really no preference. We can even simply use piece-wise linear interpolation.

3.2. Distance Functions

We observe that scutoids could be viewed as shapes constructed from 2D Voronoi diagrams that are stacked on top of each other. The shapes of the scutoids result from changes of the polygonal topology of the 2D Voronoi diagrams as we move along each interpolated plane ($z = c$). In particular, edges of Voronoi cell polygons in different layers either collapse or split by changing vertex valences. To formalize this observation, we need to show that there actually exists a formal distance function that can produce such layer by layer 2D Voronoi diagrams. In this part, we demonstrate that this distance function actually exists.

3.2.1. Generalized Distance Function

Let $\mathbf{v}$ be a vector between two points and $L_m(\mathbf{v})$ be any linear function with $m = 0, 1, \ldots, M-1$. It has been shown that the following generalization of Minkowski distance functions can be used to compute distance between any two points (36):

$$d(\mathbf{v}) = \left(\sum_{m=0}^{M-1} ||L_m(\mathbf{v})||^p \right)^{\frac{1}{p}} \tag{1}$$

where M is the number linear functions. To simplify the discussion, we assume that the linear function L_i takes the form:

$$L_i(\mathbf{v}) = \frac{\mathbf{n_m} \cdot \mathbf{v}}{s_m} \tag{2}$$

Here, $\mathbf{n_m}$ is a unit vector and $s_m > 0$.

3.2.2. Circular Disk Distance Function

Let us now consider a specific distance function in 3D where $L_0(\mathbf{v}) = x$, $L_1(\mathbf{v}) = y$, $L_2(\mathbf{v}) = z/s$, and $p = 2$, which gives us

$$d(x, y, z) = \lim_{s \to 0} \sqrt{x^2 + y^2 + \frac{z^2}{s^2}} \tag{3}$$

In this case, the implicit shape $d(x, y, z) = 1$ is an ellipsoid that will ultimately go to an infinitely thin circular disk as s tends to zero. Unfortunately, $s = 0$ will not lead to a valid distance function since $d(0, 0, 0)$ must be zero for a norm and z/s is undefined when both z and s are zero. On the other hand, if s is arbitrarily close to zero, z/s is still zero when $z = 0$.

An important interpretation of this circular disk distance is that any two points in the same layer are closer to each other than to points in layers above or below s amount since $d(0, 0, z) > d(x, y, 0)$ for $(x, y) \in [0, 1]^2$ and $|z| > s$. This is a big advantage since we now can reduce the problem of searching for equidistant boundaries in thin rectangular layers bounded by s in z and 0 and 1 in x and y. Assume that the domain consists of N layers in z direction and $s = 1/N$. Then, every layer will be given by an implicit equality as $is \geq z \geq (i + 1)s$ with $i = 0, 1, \ldots, N - 1$. We also assume that the intersection of each curve with any given layer will always be confined by a circle with radius $\sqrt{2}s$. This can easily be obtained by choosing the tangent direction never makes more than 45^0 with z direction. We also assume that highest frequency of the control curves never exceeds Nyquist limit (37). Then, we can safely sample the curves at $z = s(k+0.5)$ to use $x_i = f_{i,x}(s(k+0.5))$, $y_i = f_{i,y}(s(k + 0.5))$ as 2D Voronoi sites and we can view this decomposition as a discretization of the cubical domain into N number of 2D domains given as $z = s(k + 0.5)$.

In other words, under the assumption that the 3D structure is *thin* (as characterized by the discussion above), the 3D Voronoi decomposition reduces to 2D Voronoi decomposition of points. These assumptions can be safely imposed in a scenario where a user is designing the interpolating curves and the number of samples. This distance function significantly simplifies especially the construction of the resulting 3D shapes by converting the computation of 3D Voronoi decomposition of lines into 2D Voronoi composition of points. Based on this distance function, the construction can be done in real time during interactive design. In order to develop an intuitive design methodology for shape design, we use Delaunay diagrams.

3.3. Delaunay Diagram

It has been shown that the computation of a Voronoi diagram can be greatly simplified by working with its dual, which is known as the Delaunay diagram of the given sites (38; 39; 40). Figure 4 shows the construction of a Voronoi diagram using the Delaunay diagram. Delaunay diagrams also turn out to be useful for designing the proposed Delaunay Lofts since the problem of interpolations of polygons simplifies into that of merely interpolating points along a set of control curves. With Delaunay diagrams we can precisely design the control curve as an interpolation curve that goes through a set of critical points that defines exact locations where the polygonal topology changes.

3.3.1. Cyclic Polygons

The key idea behind Delaunay diagram are cyclic polygons. To precisely control polygonal topology changes, we use the fact that when n-number of points forms are inscribed in a circle, they form a convex cyclical polygon and their n-perpendicular bisectors to the sides are always concurrent and the common point is always the center of the circle (Figure 4(b)). This property helps us to design desired control curves by directly controlling the number of sides and vertex valances of a Voronoi tessellation in every layer. We basically create the desired Delaunay diagrams in some layers and interpolate their vertex positions. The only issue is to keep the number of vertices identical.

3.3.2. Diagram vs. Triangulation

We want to point out that Delaunay diagrams are not exactly Delaunay triangulations. Specifically, a triangulation of $n \geq 2$ sites is Delaunay if and only if the circumcircle of every interior triangle is point-free (40). One well-known but misleading property of Delaunay triangulations is that when four or more points are on the same circle, we can still create a formal Delaunay triangulation by triangulating these faces since any of these non-unique triangulations still satisfy the two properties of Delaunay triangulations. Delaunay diagrams are the real dual structures of Voronoi diagrams wherein a face becomes a vertex and a vertex becomes a face (Figures 4(c) and 4(d)).

In a Delaunay diagram, we draw only one polygon per unique circle. Not only does this eliminate any ambiguity but also simplifies the design process since the number of sides of the polygon directly defines the valence of corresponding Voronoi vertex. In the rest of this section, we discuss a few strategies to design Delaunay triangulations.

An important implication of this observation is explicit controlling topology changes. In a Delaunay triangulation, if more than one triangle share the same circle, the corresponding triangulation is not unique since it means more than three Delaunay vertices form a cyclic polygon. The number of vertices of these cyclic polygons directly determines the valance of corresponding vertex in Voronoi structure. Therefore, by controlling how many triangles share the same circle in every layer, we can change mesh topology in any desired layer.

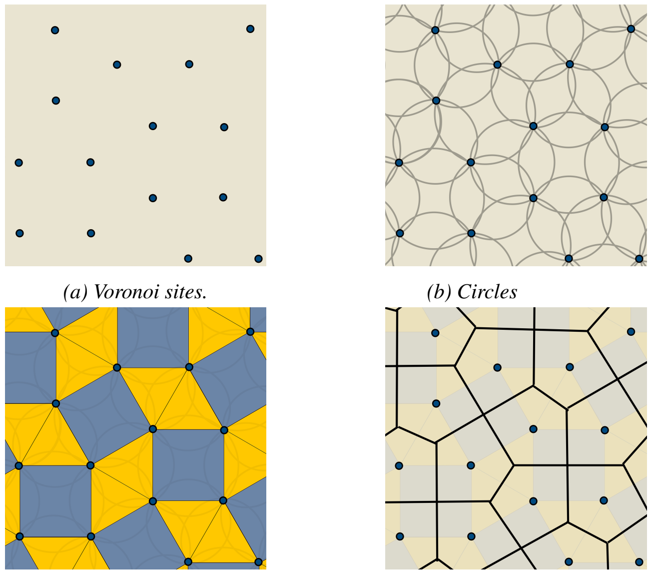

(a) Voronoi sites. *(b) Circles*

(c) Delaunay diagram. *(d) The corresponding Voronoi Diagram.*

Figure 4: An example to demonstrate how to design single polygon tilings as dual meshes of regular or semi-regular tilings. Note that each polygon in semi-regular Delaunay diagram is regular, and therefore, cyclic. (c) shows a Delaunay diagram that is a semi-regular mesh with the same vertex figure, which is 3.4.3.4.3. The corresponding Voronoi Diagram in (d) is a tiling that consists of the same polygons, which are pentagons. This property holds for all semi-regular tilings.

3.4. Regular and Semi-regular Tilings

To construct Delaunay diagrams, we are interested in geometric regularity since we want to establish cyclic conditions. Since any regular polygon are also a cyclic polygon, any tiling that consists of regular polygons are good candidates to design Delaunay diagrams.

The most obvious candidates are Euclidean regular tilings, which are planar polygonal tilings where all faces are regular polygons and all vertices are isomorphic to each other. The Schläfli symbol (n, m) is used to characterize these regular tilings, where n is the number of the sides in each face and m is the valence of vertices. There are only three regular tilings: $(3, 6)$, $(4, 4)$, and $(6, 3)$, which are regular triangular, square, and regular hexagonal tiles (41; 16). The tilings shown in Figure 2 are, in fact, the result of a bi-directional interpolation between $(6, 3)$ and $(4, 4)$ regular tilings (i.e. we have three planes in the order: $(6, 3)$, $(4, 4)$, and a translated $(6, 3)$).

If we relax the conditions of regularity, we obtain semi-regular tilings, in which all vertices have exactly the same structure and all faces are regular, but more than one type. These are usually represented with extended Schläfli symbol as a series of numbers separated by periods, where each number represent the sides of regular polygons around the vertex (42; 43; 44). For instance, 3.4.3.4.3 is a semi-regular tiling that consists of one regular triangle, one square, one regular triangle, another square and another regular triangle in a rotation order around each vertex (Figure 4(c)). In plane, there are only eight distinct semi-regular tilings. Note that duals of these semi-regular tilings consists of single polygon, not necessarily regular (Figure 4(d)). When we use these semi-regular tilings as Delaunay diagrams, we guaranteed to obtain Voronoi diagrams that consists of same type of polygons. For instance, the space filling Delaunay Loft shown in Figure 5 is designed by interpolating 3.4.3.4.3 with regular square tiles.

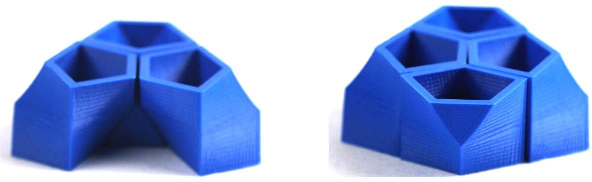

Figure 5: Another 3D printed space filling Delaunay Loft that is obtained by interpolating two 3.4.3.4.3 patters.

A generalization of regular or semi-regular tilings are k-uniform tilings, where k refers the number of different polygons (45; 46). Each can further be grouped by the number m of distinct vertex figures, which are also called m-Archimedean tilings. Regular and semi-regular tilings are 1-uniform 1-vertex tiles, i.e. there are $8 + 3 = 11$ 1-uniform tiles. Up to $k = 6$, k-uniform tiles are enumerated. For instance, we know that there are 20 2-uniform and 2-vertex tiles; 22 3-uniform and 2-vertex tiles; and 39 3-uniform and 3-vertex tiles so on. In other words, we already have an extensive list of tilings that can be constructed by regular polygons and *they all can be used as Delaunay diagrams*. The list even up to $k = 6$ is exhaustive and provides significant amount of possibilities. Also note that the cyclic condition of Delaunay is much more relaxed condition than regularity condition. It could, therefore, be better to approach the design problem using wallpaper patterns.

3.5. Wallpaper Patterns

There exist seventeen distinct symmetries in 2D plane, called wallpaper patterns. In literature, these periodic symmetry groups are called as *p1, p2, p4, pm, pmm, p4m, p4m, cm, cmm, pg, pmg, pgg, p4g, p3, p6, p3m1, p31m* and *p6m* (44). Each one of these symmetry groups is a collection of isometric operations, which preserve the distance of any two points, i.e. translation, rotation, reflection and glide reflection. The rotations can have periods two, three, four or six. The complete list of the 17 symmetry groups in plane can be classified in two categories: rectangular and hexagonal. Namely, 12 of these 17 groups have rectangular symmetries, i.e. their natural fundamental domain is a rectangle. The remaining 5 have hexagonal symmetries, i.e. their natural fundamental domain is a hexagon.

It has been shown that we can use rectangle as the fundamental domain for hexagonal symmetries (47). In other words, regardless of the symmetry group, any symmetric tiles can be represented by a simple rectangular fundamental domain, which can be embedded over a toroidal surface. Thus, we can construct any wallpaper by symmetry operations that is constrained in fundamental domain.

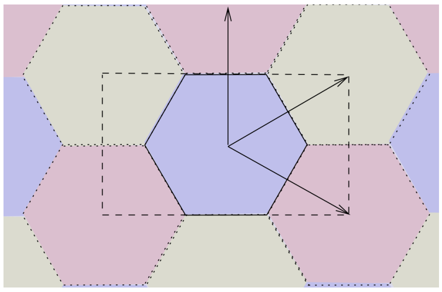

Figure 6: Rectangle can also be used as a fundamental domain for the five wallpaper symmetries whose natural fundamental domain is a regular hexagon (47).

This property is not just practically useful for our application, it also provides the theoretical support to use cubical fundamental domain for Delaunay Lofts. Because of this property, we can obtain any 2D wallpaper symmetrical Voronoi decomposition that can be obtained using points as Voronoi sites in any layer. Control curves can simply be obtained by interpolating Voronoi sites (i.e. Delaunay vertices).

Another important property of wallpaper patterns, which we use, is that all semi-regular tilings can be constructed using wallpaper symmetry operations. In a semi-regular tiling the vertices being “the same” means that for every pair of vertices there is a symmetry operation. For instance, in semi-regular mesh 3.4.3.4.3 has the wallpaper symmetry *p4g*.

The only caveat in this approach in terms of the design is that the number of Voronoi sites in every layer has to be the same. Using a rectangle as our regular domain also provides a solution to that problem. Note that the regular rectangular domain in Figure 6 actually consists of two hexagons, one full (blue), and a second one that is decomposed into four pentagons (two yellow and two red). This means that if we create points in hexagonal symmetry, we need to multiply the number of points by two. Also note that the symmetries always have periods of either two, three, four or six. Using this information, we obtain the same number of points using their least common multiples (LCM). For instance, if we want to connect symmetries with four or six, 12 points will be sufficient. One will be created as three random points with four period. Another will be created as one random point with period six in two hexagons.

4. Methodology

The key element of our approach is a distance function that reduces Voronoi decomposition for a given set of curves into a set of Voronoi decomposition with respect to points on those curves. This approach makes the our construction algorithm independent of the complexity of the control curve while providing well-defined and curved boundaries. Based on our construction algorithm, we have also developed an intuitive methodology to design these structures. We simply produce the control curves as an interpolation of the vertices of the a set of stacked Delaunay diagrams, i.e. vertices of the dual graphs of a set of stacked 2D Voronoi diagrams, with the same number of vertices. The Voronoi decomposition obtained with these control curves gives us a natural interpolation of 2D Voronoi diagrams producing Delaunay Lofts.

An important implication of this approach is that it allows us to explicitly control topological changes across the evolving Voronoi decomposition. In a Delaunay triangulation, if more than one triangle share the same circle, the corresponding triangulation is not unique since it means more than three Delaunay vertices form a cyclic polygon. The number of vertices of these cyclic polygons directly determines the valance of corresponding vertex in Voronoi structure. Therefore, by controlling how many triangles share the same circle in every layer, we can change mesh topology in any desired layer.

4.1. Construction Methods

We present a construction algorithm in a domain of bounded rectangular prism and extend this construction algorithm for rectangular prisms that are fundamental domains.

4.1.1. General Construction Algorithm

The process consists of the following steps:

1. Sample N number of constant z planes for a rectangular prism. We call these planes layers, as shown in Figure 7(a).
2. Design M number of curves inside of the rectangular domain. Figure 7(b) is an example using randomly generated line segments using jittered points on the extremal layers.
3. Find the intersection of curves with intermediate layers. For each layer, compute its Voronoi partitioning by using intersection points with that particular layer as Voronoi sites. Since the space is bounded, the boundaries of the prism becomes part of Voronoi polygons (See Figure 7(c)).
4. Offset each Voronoi polygon the same amount using Minkowski difference. Note that this process can also change topology of the polygons (See Figures 7(d,e)).
   Remark: Step 4 ensures the production of separable Delaunay Lofts while printing a tiling as a whole. The offset is half the width of the 3D printing nozzle.
5. Treating each vertex as a single manifold, insert edges between consecutive vertices thereby turning each original face into a 2-sided face, which is 2-manifold (48) (See Figure 7(f)).
6. Connect 2-sided faces with insert-edge operations (49) to form a single genus-0 object (See Figure 7(g)). This series of edge insertions results in a Delaunay Loft (See Figure 7(h)).

4.1.2. Construction of a Single Delaunay Loft

Here, we present an algorithm that guarantees to obtain genus-0 surface that corresponds to a single Delaunay Loft.

1. For every two consecutive 2-sided faces, select the polygons they face each others. Each of these polygons will be given a set of half-edges with opposing rotation orders. Figure 8(a) provides an example of such two such polygons, one triangle and one pentagon. Note that the rotation order of half-edges in the triangle is counter-clockwise and rotation order of half-edges in the pentagon is clockwise.
2. Compare vertex positions of the two polygons and identify two closest vertices.
3. Insert an edge between the corners of two closest vertices of the two polygons (See Figure 8(b)). Insert edge operation combines the two planar polygons into one face. When we complete this operation for all pairs of polygons, the resulting structure is a single genus-0 surface. The only problem is that the resulted combined faces are complicated with one edge whose both half-edges are in

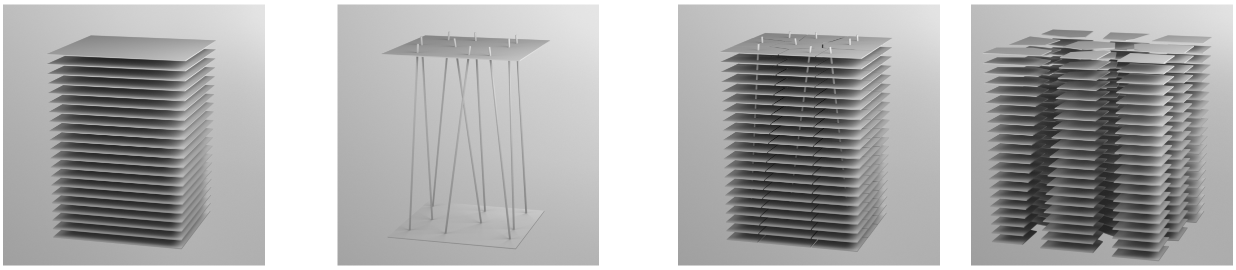

(a) Initial Layers. *(b) The control curves.* *(c) Voronoi decomposition of layers.* *(d) Offset polygons.*

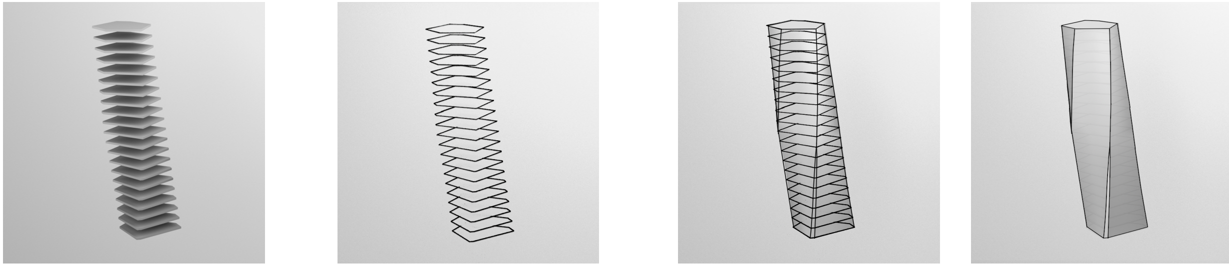

(e) Offset polygons for one Voronoi Loft. *(f) Construction of 2D sided (i.e. 2-manifold) faces.* *(g) Connecting 2-sided faces by inserting edges.* *(h) Final Voronoi Loft.*

Figure 7: Construction Algorithm over a bounded rectangular prism domain.

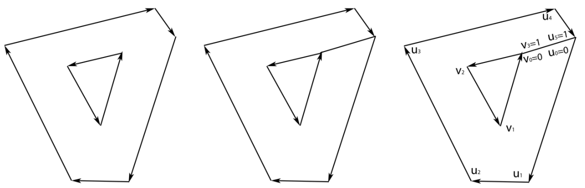

(a) Initial polygon-pair with opposite rotation order *(b) Inserting an edge to combine the two polygons* *(c) Parametrization of corners of combined face*

Figure 8: An example of connecting two polygons, a pentagon and and a triangle, by inserting edges. Half-edges are shown as arrows and edges (i.e. two half-edges) are shown as line segments.At the end of a process of a series of edge insert operations, we obtain triangles and quadrilaterals by subdividing combined face.

the same face. Therefore, there is a need for subdividing this face into geometrically well-defined faces, i.e. triangles and quadrilaterals.

Remark: It is easy to subdivide the combined face using a series of insert edge operations. Since an insert edge operation that is applied to a 2-manifold mesh always creates another 2-manifold, we can never get non-manifold. On the other hand, if one is not careful, it is always possible to introduce topological noise, i.e. one can increase genus by introducing holes and handles (50). Next step provides an algorithm to avoid that guarantees genus-0 surface.

4. Assign two parameters, $0 \geq u \geq 1$ and $0 \geq v \geq 1$, along the perimeter of each polygon, one in counter-clockwise and another in clockwise, starting from one side of the inserted edge and ending the other side of inserted edge. This assigns a parametric position to each corner of the polygon u_i and u_j as follows:

$$u_n = \frac{1}{L}\sum_{i=0}^{n-1} L_i \ , \quad v_m = \frac{1}{D}\sum_{i=0}^{m-1} D_i \tag{4}$$

where L_i and D_i are length of half-edges in polygons 1 and 2 respectively; $L = \sum_{i=0}^{N-1} L_i$, $D = \sum_{i=0}^{M-1} D_i$, and $N \geq M$.

5. To guarantee that the operation does not produce topological noise, i.e. not to increase genus, edges must be inserted between corners in the same face. This could be done a variety of the ways. The following pseudo-code provides the algorithm we use to obtain genus-0 Delaunay Lofts:

4.1.3. Construction with Fundamental Domain

This extension is straightforward. We use nine copies of fundamental domain to form a single rectangular prism and compute Delaunay Lofts as in previous subsection. However, we only use Delaunay Lofts in the center rectangular prism .

Algorithm 1: Pseudocode for Single Delaunay Loft

n = 0; m = 0;
while *($n \leq N$ and $m < M$) or ($n < N$ and $m \leq M$)* **do**
  if *($n < N$)* **then**
    n = n++;
  if *($|u_n - v_m| \leq |u_n - v_{m+1}|$)* **then**
    InsertEdge(u_n, v_m);
  else
    InsertEdge(u_n, v_{m+1});
    if *($m < M$)* **then**
      m++;

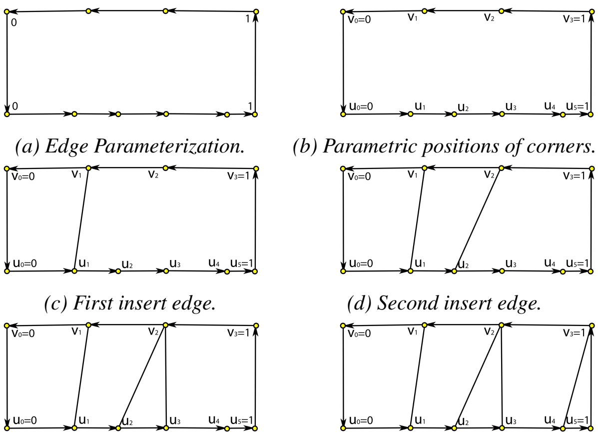

(a) Edge Parameterization. *(b) Parametric positions of corners.*
(c) First insert edge. *(d) Second insert edge.*
(e) Forth insert edge. *(f) Fifth insert edge.*

Figure 9: The algorithm in parameter domain working for the example shown in 8, showing parametric positions of u_n's and v_m's.

5. Results

Our approach when applied to the original scutoid discovered by Gomel-Gomez et al. (mapping Hexagon to Pentagon) (7) produces curved surfaces which is different from the common description of scutoids with planar surfaces (Figure 3). Note that not more than 4 of these shapes can fit together to create a repeatable block. In our approach, the interface between any two shapes are naturally curved due to Voronoi-based interpolation ensuring that the tiling is space-filling.

The construction algorithm allows for exploring and investigating a vast variety of shapes that are possible now. The only constraint is to have the total number of points to be equal in the two layers we intend to interpolate. To ensure repeatability of the Delaunay Lofts, we should have geometric regularity in the tilings we interpolate. In the following sub-sections, we explore different strategies for achieving the geometric regularities. Furthermore, for a few selective cases, we also conducted preliminary finite element analysis (FEA) to better understand the potential advantages of Delaunay Lofts over prisms.

5.1. Delaunay Lofts with 464

Since any regular polygon is also a cyclic polygon, we start with regular polygon tilings as they are good candidates to design Delaunay diagrams. We will then extend and generalize this idea to Semi-regular and Regular tilings with Wallpaper patterns. We start our exploration with a simple Hexagonal tiling, which is one of the three Euclidean tilings of the space (apart from square and triangle). With the longer axis of the hexagon aligned vertically, we move alternate rows of hexagon tiling in opposite directions. We displace the Hexagon by an amount equal to half the horizontal distance between two subsequent cells in a row. Half way through the process, every hexagon changes to a quadrilateral. Similar interpolation pattern was also suggested by Kaplan (25) in his work on Voronoi Diagrams and ornamental design.

We conducted a preliminary FEA on the 464 Delaunay Loft with the hypothesis that since the central layer ($z = 0.5$ in parametric domain) is enforced to be a regular quadrilateral tiling, we will observe some interesting effects at this layer when compression, tension and torsion are applied individually to a single 464-Loft (Figure 10). This indeed turned out to be true. The analysis shows that the stress levels are lower in the regions where the topology changes (vertex-split and edge-collapse occurs). We suspect that these mechanical properties are likely as scutoids are proved to stabilize the three-dimensional packing and minimize the tissue-energy based on biophysical arguments as proposed by Gomel-Gomez et al (7). A detailed and systematic investigation is needed to confirm this hypothesis.

A simple extension to regular hexagon interpolation by reducing the distance in between the cells on the extremal layers would give us a Quad - Quad interpolation (Figure 2), with again a Quad in the center. We also found another interesting case similar to the T1 transition (51) that occurs during the morphogenetic process. We patterned one such transition throughout the plane to obtain the Pent-Quad-Pent shapes (Figure 12). Similar to previous examples these have lower stress at the critical points where the topology changes in the FEA results for twisting, compression and shear (Figure 10).

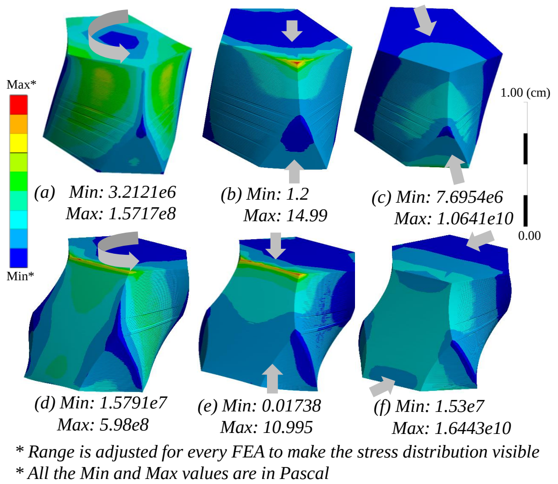

Figure 10: Contour-Maps of Equivalent Stress (von-Mises) of two Delaunay Lofts (Pent-Quad-Pent on top row, Hex-Quad-Hex on bottom row) are shown for three loading conditions, namely, torsion (a, d), compression (b, e), and shear (c, f). In all cases, the stress distribution decreases around the critical points where the topology changes. The torque and compression stress were 1 Nm and 1 Pa respectively. The Lofts were sheared by displacing the top layer by 0.1 mm with a fixed bottom layer. All simulations were done using ANSYS® Mechanical Enterprise (ANSYS 2019 R1).

5.2. Investigating Wallpaper Symmetry

Here, we generalize beyond the special cases discussed in the previous section to generate more planer symmetries based on one of the 17 wallpaper groups. We start with $p4$ symmetries wherein we take a subdivide a unit square into 4 equal square pieces and sample points with 4 rotational symmetry. By extending this symmetry to the control curves in 3D space (achieved simply by mirroring the selected control curves about the z direction), we can simply repeat the unit domain in 3D space to construct the tilings. Most of the Delaunay Lofts we get using these symmetry patterns have highly curved interfacing between two adjacent tiles and may offer better interlocking capabilities when compared with its prism counterparts. We can also extend the tilings to semi-regular tilings. We have shown few results in which two Delaunay Lofts together fill the space in a specific pattern (Figure 13).

5.3. Extension to Curved Control Lines

Extending our method to non-linear control curves, such as circular, cosine, or Hermitian, is especially promising for creating more unusual free-form tilable shapes. We specifically experimented with Hermitian interpolation (Figure 11) since it is possible to extend this to multiple control layers and more control in derivatives. Note that we do not have to be careful to keep the curves in the rectangular prism domain since the curves are conceptually drawn in 3-torus.

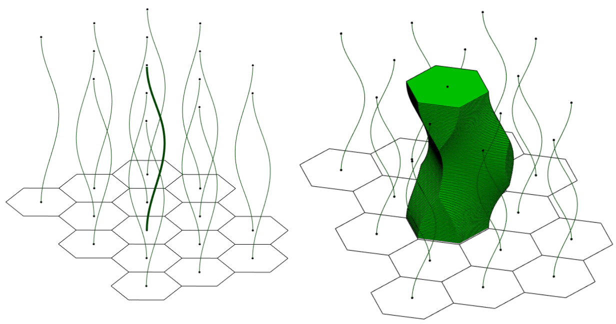

Figure 11: A space filling Delaunay Loft obtained by Hermitian curves.

6. Discussion

6.1. Geometric Properties & Tilings

Broadly speaking, there are two main geometric requirements that was needed from the 3D shapes that we intended to create. First, we wanted to be able to compose space filling patterns with the shapes. Second, we hoped for the pattern to be composed of ideally a single (or at least a finite set of) repeatable shapes. Here, our approach offered a unique advantage. The first condition is naturally satisfied by the strategy to use Voronoi partitioning (since any such partitioning is guaranteed to fill space of any given dimension). Therefore, the space filling condition is satisfied regardless of how the Voronoi sites are distributed on each of the extremal surfaces (as long as we can establish a on-to-one correspondences between the sites on each surface). We then addressed the second condition of repeatability through our method of construction and design based on wallpaper symmetries. Combining these two components resulted in a simple yet powerful methodology.

Most works on tiled 3D shapes in the past are performed purely by geometric reasoning. We believe that this change of perspective offered a unique advantage. Ours is probably the first to apply geometric reasoning to describe a bio-physical phenomenon in order to apply it to 2.5D tiling design in a systematic manner. Our approach provides a possible explanation for the occurrence of scutoids in skin cells (7) and demonstrates the construction of many other shapes similar to scutoids.

Having said this, we would also like to point out that it is still to be completely tested that the method that

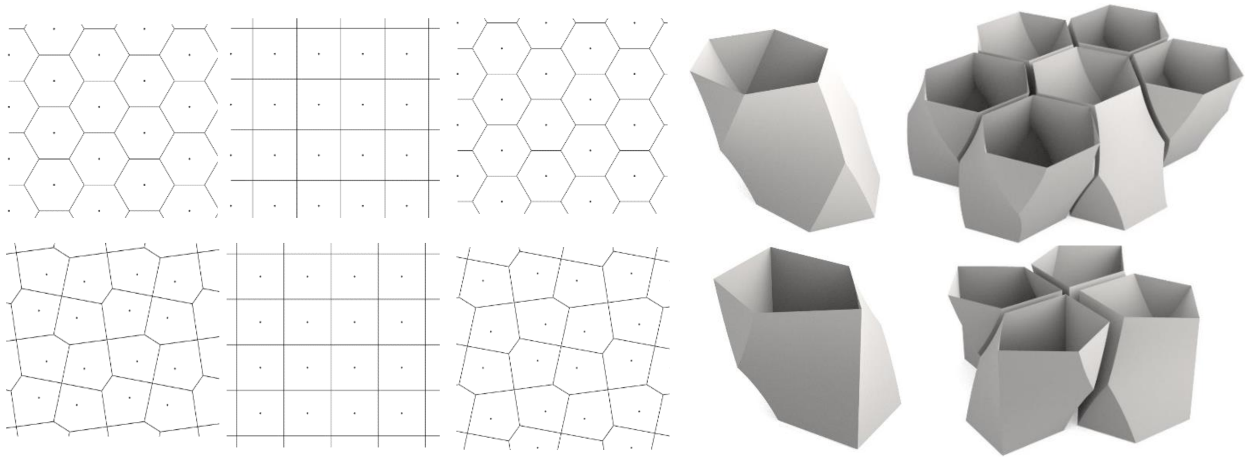

Figure 12: The three patterns (left to right) show the Voronoi diagrams from the bottom, middle and the top layer of interpolation. In the first row we show the 464 Delaunay Lofts and second row shows the Delaunay Lofts obtained by interpolating 3.4.3.4.3 patterns.

we propose here for constructing Delaunay Lofts can indeed also be used to model the original scutoids. The key gap that needs to be addressed for this is to compare the actual geometry (and not the idealized model shown in Figure 3) that is experimentally obtained with one constructed using our approach with the same initial conditions as the bio-physical case.

6.2. *Geometric Design Space*

The design space of shapes that can be composed using our approach is unusually rich. This is due to three facts. First, the construction algorithm does not assume any specific shape of the control curves — as long as they intersect each slicing plane at a unique point thus maintaining the number of sites per slice. This alone provides many possibilities in terms of obtaining seemingly complex geometries. Second, the 17 wallpaper symmetries result in several possibilities in terms of the tiling configurations that may be possible with our approach. Finally, the distance functions utilized in all our examples are only L^2-norms. Generalizing to L^p-norms will lead to even more unusual shapes that we have currently demonstrated. Having said this, we have currently exposed only a limited set of repeatable tiles as examples in the paper. We are currently developing a more systematic geometric kernel and interactive software to explore the complete design space of Delaunay Lofts.

7. Conclusion and Future Work

In this paper, we presented an approach to construct and eventually design a new class of tilings in 3D space. We have developed an algorithm that takes as input two planes containing Voronoi tessellations based on some distribution of points and interpolates the tilings between these given planes. The volumetric structures obtained through this interpolation result in the occurrence of Delaunay Lofts. There are several variations of how this interpolation can lead to a variety of such Lofts.

The future work is to investigate the power of shapes that are created by our bio-inspired design approach in terms of withstanding stress, torsion or fatigue. If these approaches can create powerful shapes in terms of withstanding stress , torsion and fatigue, this approach could be arguably applied to come up with completely new designs and structures that could have greater strength. An advantage of our approach is that it can easily be used in combinatorial optimization. Therefore, this approach could take the industry to the next level of material optimization and unveil endless possibilities of geometric designs with Delaunay Lofts.

8. Acknowledgments

We thank the reviewers for their valuable feedback and comments. This work was supported by the Texas A&M Engineering Experiment Station and the J. Mike Walker '66 Department of Mechanical Engineering at Texas A&M University.

[1] E. Whiting, J. Ochsendorf, F. Durand, Procedural modeling of structurally-sound masonry buildings, ACM Trans. Graph. 28 (5) (2009) 112:1–112:9. doi:10.1145/1618452.1618458.

[2] M. Deuss, D. Panozzo, E. Whiting, Y. Liu, P. Block, O. Sorkine-Hornung, M. Pauly, Assembling self-supporting structures, ACM Trans. Graph. 33 (6) (2014) 214:1–214:10. doi:10.1145/2661229.2661266.

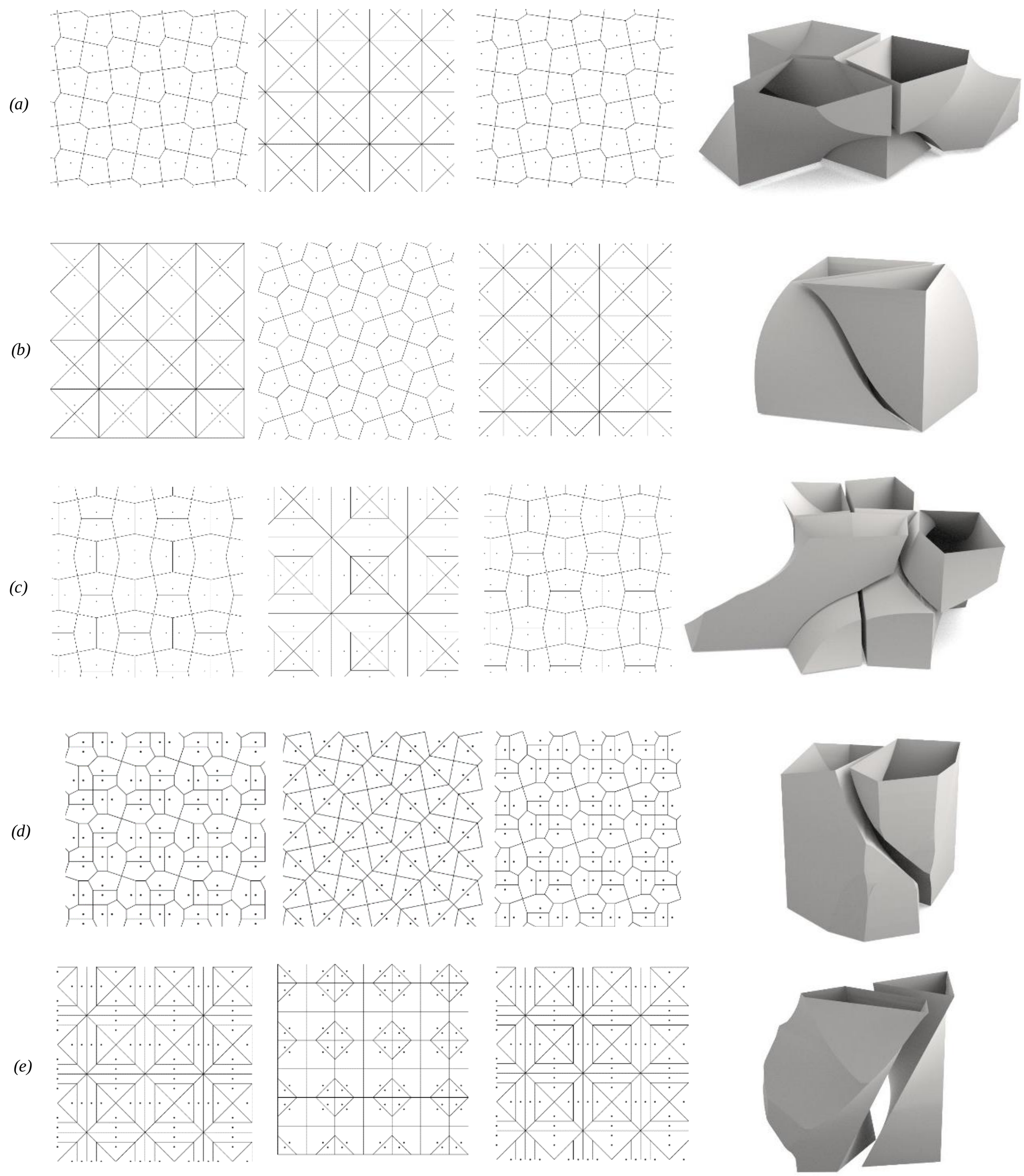

Figure 13: This figure shows five more Delaunay Lofts got by applying wallpaper symmetry patterns to the control curves in 3D. In each row, we show the transition of Voronoi from the bottom layer, middle layer and the top layer followed by the corresponding tiling we get. We specifically leave small gaps between the Delaunay Lofts to appreciate how nicely the shape fit well with each other. Figure (a) shows a transition from Pentagon in the Top and bottom layer with a Triangle in the middle. (b) shows Triangle on top and bottom with a Pentagonal Middle layer. The Delaunay Lofts (c), (d) and (e) however go through a series of transitions within Triangle, Quadrilateral and Pentagonal layers. This is the reason for the intricate shapes of these Lofts. Some of the symmetry patterns in 2D were also inspired from Kaplan's work on Ornamental design using Voronoi diagram (25).

[3] E. Whiting, H. Shin, R. Wang, J. Ochsendorf, F. Durand, Structural optimization of 3d masonry buildings, ACM Trans. Graph. 31 (6) (2012) 159:1–159:11. doi:10.1145/2366145.2366178.

[4] H. V. Shin, C. F. Porst, E. Vouga, J. Ochsendorf, F. Durand, Reconciling elastic and equilibrium methods for static analysis, ACM Trans. Graph. 35 (2) (2016) 13:1–13:16. doi:10.1145/2835173.

[5] M. Kilian, D. Pellis, J. Wallner, H. Pottmann, Material-minimizing forms and structures, ACM Trans. Graphics 36 (6) (2017) article 173, proc. SIGGRAPH Asia. doi:http://dx.doi.org/10.1145/3130800.3130827.

[6] G. Fallacara, Toward a stereotomic design: Experimental constructions and didactic experiences, in: Proceedings of the Third International Congress on Construction History, 2009, p. 553.

[7] P. Gómez-Gálvez, P. Vicente-Munuera, A. Tagua, C. Forja, A. M. Castro, M. Letrán, A. Valencia-Expósito, C. Grima, M. Bermúdez-Gallardo, Ó. Serrano-Pérez-Higueras, et al., Scutoids are a geometrical solution to three-dimensional packing of epithelia, Nature communications 9 (1) (2018) 2960.

[8] A. L. Loeb, Space-filling polyhedra, in: Space Structures, Springer, 1991, pp. 127–132.

[9] B. Grünbaum, G. C. Shephard, Tilings with congruent tiles, Bulletin of the American Mathematical Society 3 (3) (1980) 951–973.

[10] M. Senechal, Which tetrahedra fill space?, Mathematics Magazine 54 (5) (1981) 227–243.

[11] M. Gardner, Sixth book of mathematical games from Scientific American, WH Freeman San Francisco, 1971.

[12] M. Goldberg, The space-filling pentahedra, Journal of Combinatorial Theory, Series A 13 (3) (1972) 437–443.

[13] M. Goldberg, Convex polyhedral space-fillers of more than twelve faces, Geometriae Dedicata 8 (4) (1979) 491–500.

[14] M. Goldberg, On the space-filling enneahedra, Geometriae Dedicata 12 (3) (1982) 297–306.

[15] R. E. Williams, Space-filling polyhedron: its relation to aggregates of soap bubbles, plant cells, and metal crystallites, Science 161 (3838) (1968) 276–277.

[16] R. Williams, The geometrical foundation of natural structure: A source book of design, Dover New York, 1979.

[17] N. W. Johnson, Convex polyhedra with regular faces, Canadian Journal of Mathematics 18 (1966) 169–200.

[18] S. Alvarez, The gyrobifastigium, not an uncommon shape in chemistry, Coordination Chemistry Reviews 350 (2017) 3–13.

[19] H. S. M. Coxeter, Regular polytopes, Courier Corporation, 1973.

[20] T. W. Sederberg, E. Greenwood, A physically based approach to 2–d shape blending, ACM SIGGRAPH computer graphics 26 (2) (1992) 25–34.

[21] T. W. Sederberg, P. Gao, G. Wang, H. Mu, 2-d shape blending: an intrinsic solution to the vertex path problem, Proceedings of the 20th annual conference on Computer graphics and interactive techniques (1993) 15–18.

[22] M. Alexa, D. Cohen-Or, D. Levin, As-rigid-as-possible shape interpolation, in: Proceedings of the 27th annual conference on Computer graphics and interactive techniques, ACM Press/Addison-Wesley Publishing Co., 2000, pp. 157–164.

[23] G. Turk, J. F. O'brien, Shape transformation using variational implicit functions, in: ACM SIGGRAPH 2005 Courses, ACM, 2005, p. 13.

[24] C. Schumacher, S. Marschner, M. Cross, B. Thomaszewski, Mechanical characterization of structured sheet materials, ACM Trans. Graph. 37 (4) (2018) 148:1–148:15. doi:10.1145/3197517.3201278.

[25] C. S. Kaplan, Voronoi diagrams and ornamental design, in: in The First Annual Symposium of the International Society for the Arts, Mathematics, and Architecture, 2000, pp. 277–283.

[26] M. Rao, Exhaustive search of convex pentagons which tile the plane, arXiv preprint arXiv:1708.00274 (2017).

[27] H. Honda, Description of cellular patterns by dirichlet domains: The two-dimensional case, Journal of Theoretical Biology 72 (3) (1978) 523 – 543.

[28] G. Blanchard, A 3d cell shape that enables tube formation (2018).

[29] C. M. Nelson, Epithelial packing: Even the best of friends must part, Current Biology 28 (20) (2018) R1197–R1200.

[30] A. Mughal, S. Cox, D. Weaire, S. Burke, S. Hutzler, Demonstration and interpretation of" scutoid" cells in a quasi-2d soap froth, arXiv preprint arXiv:1809.08421.

[31] B. N. Delaunay, N. N. Sandakova, Theory of stereohedra, Trudy Matematicheskogo Instituta imeni VA Steklova 64 (1961) 28–51.

[32] M. W. Schmitt, On space groups and dirichlet–voronoi stereohedra, Ph.D. thesis, Berlin: Freien Universitt Berlin (2016).

[33] J.-P. Luminet, B. F. Roukema, Topology of the universe: Theory and observation, in: Theoretical and Observational Cosmology, Springer, 1999, pp. 117–156.

[34] E. Cohen, R. F. Riesenfeld, G. Elber, Geometric modeling with splines: an introduction, AK Peters/CRC Press, 2001.

[35] F. Massarwi, G. Elber, A b-spline based framework for volumetric object modeling, Computer-Aided Design 78 (C) (2016) 36–47.

[36] E. Akleman, J. Chen, Generalized distance functions, in: Proceedings Shape Modeling International'99. International Conference on Shape Modeling and Applications, IEEE, 1999, pp. 72–79.

[37] H. Nyquist, Certain topics in telegraph transmission theory, Transactions of the American Institute of Electrical Engineers 47 (2) (1928) 617–644.

[38] B. N. Boots, Delaunay triangles: an alternative approach to point pattern analysis, Proceedings of the Association of American Geographers 6 (1974) 26–29.

[39] D. F. Watson, Computing the n-dimensional delaunay tessellation with application to voronoi polytopes, The computer journal 24 (2) (1981) 167–172.

[40] L. Guibas, J. Stolfi, Primitives for the manipulation of general subdivisions and the computation of voronoi, ACM transactions on graphics (TOG) 4 (2) (1985) 74–123.

[41] I. Stewart, Game, set and math: enigmas and conundrums, Courier Corporation, 2007.

[42] B. Grünbaum, G. C. Shephard, Tilings by regular polygons, Mathematics Magazine 50 (5) (1977) 227–247.

[43] B. Grünbaum, G. Shephard, The ninety-one types of isogonal tilings in the plane, Transactions of the American Mathematical Society 242 (1978) 335–353.

[44] B. Grünbaum, G. C. Shephard, Tilings and patterns, Freeman, 1987.

[45] D. Chavey, Tilings by regular polygons ii a catalog of tilings, in: Symmetry 2, Elsevier, 1989, pp. 147–165.

[46] N. Lenngren, k-uniform tilings by regular polygons, www.diva-portal.org/smash/get/diva2:444746/FULLTEXT01.pdf (2009).

[47] E. Akleman, J. Chen, B. Meric, Web-based intuitive and effective design of symmetric tiles, Proceedings of ACM Multimedia 21 (4) (2000) 100–108.

[48] V. Srinivasan, E. Akleman, J. Chen, Interactive construction of multi-segment curved handles, in: Computer Graphics and Applications, 2002. Proceedings. 10th Pacific Conference on, IEEE, 2002, pp. 429–430.

[49] E. Akleman, J. Chen, V. Srinivasan, A minimal and complete set of operators for the development of robust manifold mesh

modelers, Graphical models 65 (5) (2003) 286–304.
[50] I. Guskov, Z. J. Wood, Topological noise removal, 2001 Graphics Interface Proceedings: Ottawa, Canada (2001) 19.
[51] M. Tada, C.-P. Heisenberg, Convergent extension: Using collective cell migration and cell intercalation to shape embryos, Development (Cambridge, England) 139 (2012) 3897–904. doi:10.1242/dev.073007.